BEAM-INDUCED HEATING / BUNCH LENGTH / RF AND LESSONS FOR 2012

E. Métral (for the ABP/ICE section, many collaborators and equipment groups)

Abstract

The observations made in 2011 in the LHC are first compared to expectations and the possible implications for the operation in 2012 are then discussed.

INTRODUCTION

Beam-induced heatings have been observed here and there during the 2011 run when the bunch/beam intensity was increased and/or the bunch length was reduced. These observations are first reviewed before mentioning the recent news/work performed during the shutdown. In fact, several possible sources of heating exist and only the RF heating (i.e. coming from the real part of the longitudinal impedance of the machine components) is discussed in some detail in the present paper: (i) comparing the case of a Broad-Band (BB) vs. a Narrow-Band (NB) impedance; (ii) discussing the beam spectrum; (iii) reminding the usual solutions to avoid/minimize the RF heating; (iv) reviewing the different heat transfer mechanisms; (v) mentioning that the synchronous phase shift is a measurement of the power loss and effective impedance. The three current "hot" topics for the LHC performance, which are the VMTSA, TDI and MKI, are then analyzed in detail and some lessons for 2012 (and after) are finally drawn.

2011 RUN OBSERVATIONS

All the observations are summarized in Table 1 [1], with some additional information for each equipment. From this list the two most critical equipments are the MKI and the VMTSA, which could prevent the LHC from running with higher beam intensities in 2012.

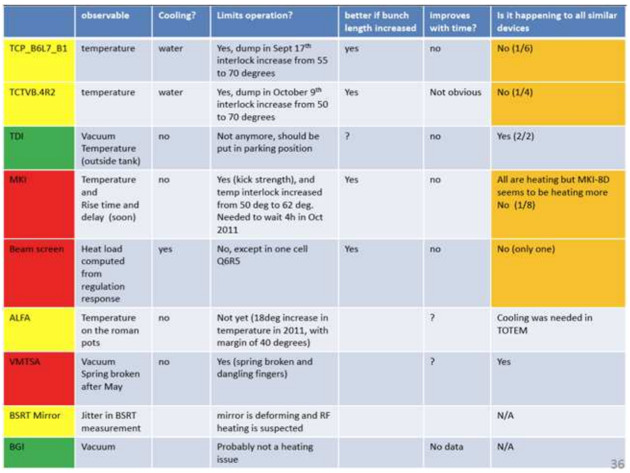

	observable	Cooling?	Limits operation?	better if bunch length increased	improves with time?	Is it happening to all similar devices
TCP_B6L7_B1	temperature	water	Yes, dump in Sept 17th interlock increase from 55 to 70 degrees	yes	no	No (1/6)
TCTVB.4R2	temperature	water	Yes, dump in October 9th interlock increase from 50 to 70 degrees	Yes	Not obvious	No (1/4)
TDI	Vacuum Temperature (outside tank)	no	Not anymore, should be put in parking position	?	no	Yes (2/2)
MKI	Temperature and Rise time and delay (soon)	no	Yes (kick strength), and temp interlock increased from 50 deg to 62 deg. Needed to wait 4h in Oct 2011	Yes	no	All are heating but MKI-8D seems to be heating more No (1/8)
Beam screen	Heat load computed from regulation response	yes	No, except in one cell Q6R5	Yes	no	No (only one)
ALFA	Temperature on the roman pots	no	Not yet (18deg increase in temperature in 2011, with margin of 40 degrees)		?	Cooling was needed in TOTEM
VMTSA	Vacuum Spring broken after May	no	Yes (spring broken and dangling fingers)		?	Yes
BSRT Mirror	Jitter in BSRT measurement		mirror is deforming and RF heating is suspected			N/A
BGI	Vacuum		Probably not a heating issue		No data	N/A

Table 1: Summary table with all the equipments where beam-induced heating was observed in 2011.

NEWS/WORK DURING THE SHUTDOWN

Several observations have been made together with some hardware modifications:

- **VMTSA**: 8 new modules have been installed (instead of the 10 of 2011) with shorter RF fingers and ferrite plates after some electromagnetic simulations and bench impedance measurements (see later).
- **TDI**: a visual inspection revealed a beam screen deformation and a very soft copper (see Fig. 1).

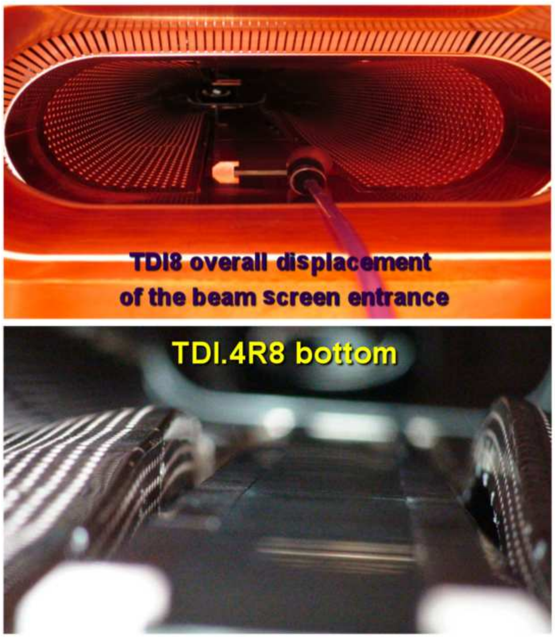

Figure 1: Pictures of the observed TDI beam-screen deformation (Courtesy of Benoit Salvant et al.).

- **TCTVB.4R2**: it has been removed during the shutdown. TCTVB.4L2 (i.e. not the most critical one) has been looked at and some RF fingers were found not in contact.
- **TCP.B6L7.B1**: nothing obvious could be revealed by visual inspection; Xrays measurements remain to be done but might be quite difficult to do.
- **Q6R5 (beam screen):** Xrays were performed but nothing special could be found.
- **ALFA, MKI and TDI**: more electromagnetic simulations have been performed.

RF HEATING

Consider the case of M equi-spaced equi-populated bunches, which should be a good approximation when the

LHC machine is full. In this case, the general formula for the beam power loss (due to the interaction with the longitudinal impedance) can be written [2]

$$P_{loss} = M \, I_b^2 \, Z_{loss} \,, \tag{1}$$

with

$$Z_{loss} = 2\, M \sum_{p=0}^{\infty} \mathrm{Re}\big[Z_l (p \, M \, \omega_0) \big] \times \mathrm{PowerSpectrum}\big[p \, M \, \omega_0 \big] \,, \tag{2}$$

where $I_b = N_b \, e \, f_0$ is the bunch current (with N_b the number of protons per bunch, e the elementary charge and f_0 the revolution frequency), $\omega_0 = 2 \pi f_0$, Z_l the longitudinal impedance, and PowerSpectrum stands for the beam power spectrum.

The scaling of this power loss with respect to the bunch intensity is thus clear (it is always quadratic), but the scaling with the number of bunches is less obvious: (i) in the case of a BB impedance, the sum in Eq. (2) can be replaced by an integral (the *M* in front then disappears; see detailed example later) and the result is that the total power loss is just *M* times the single-bunch case; (ii) in the case of (very) NB impedance, only one term in the sum is useful (assuming the worst case where the line in on top of a coupled-bunch line) and the result is that the total power loss is NOT just *M* times the single-bunch case, but it goes with the square of the number of bunches (because in this case what is important is the total beam current; see detailed example later).

As concerns the beam (power) spectrum, measurements have been performed in 2011 before the ramp and in stable beams (see Fig. 2). Figure 2 reveals interesting features, which are worth discussing a bit. First, many peaks are spaced by ~ 20 MHz (as it is expected for the 50 ns bunch spacing beam used; the bunch frequency would be ~ 40 MHz for the 25 ns beam) below an envelope which is decreasing with frequency until a certain value and which is then revealing a side lobe (and sometimes also others). This behaviour is exactly the one expected due to the finite length of the bunch (inside a finite bucket). To get a better feeling, let's consider four typical (theoretical) distributions, whose longitudinal profiles are represented in Fig. 3. The two extreme cases are, on one side the Gaussian distribution with infinite and smooth tails (therefore unrealistic) and on the other side the Water-Bag distribution with finite and sharp tails. The corresponding power spectra can be computed analytically and they are depicted in Fig. 4. It is clearly seen that only the (unrealistic) Gaussian distribution does not reveal side lobes due to the fact that the tails extend up to infinity. For all the other distributions (with finite lengths), sides lobes are revealed and the sharper the tails the higher the sides lobes. However, in the measurements the height of the first side lobe is at ~ - 35 or - 40 dB, whereas the theoretical distributions considered give higher values. This means that the real distribution must have smoother tails. Consider now a family of (finite) distributions, keeping the same half width at half height, depending on the parameter *n* (converging to a Gaussian distribution when *n* goes to infinity, see Fig. 5). The corresponding power spectra are depicted in Fig. 6. It is seen that the distribution with *n* = 3 should be a relatively good approximation (even if two side lobes are expected from theory in this case whereas only a large one was measured… maybe it is the envelope of the two…).

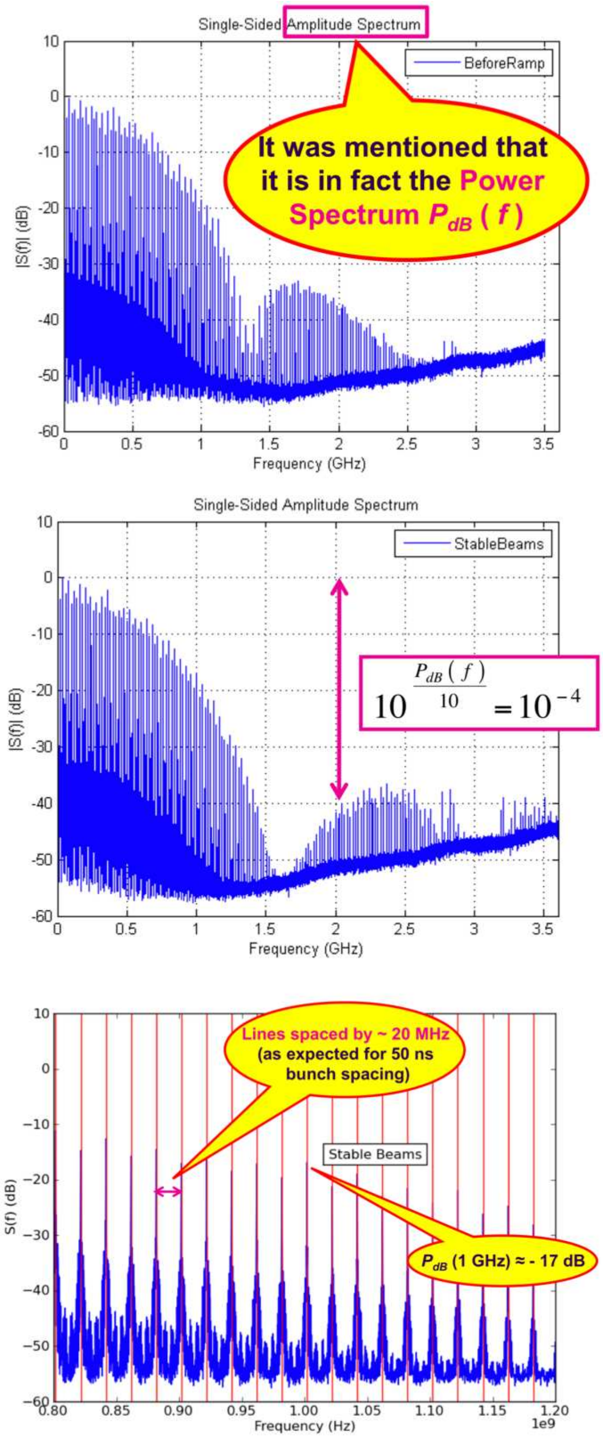

Figure 2: Power spectra measurements for beam 1 on fill # 2261 (Courtesy of Themistoklis Mastoridis, Philippe Baudrenghien and Hugo Day).

By taking the inverse Fourier Transform of the measured spectrum, the longitudinal profile of Fig. 7 has been obtained, which is consistent with the expected one from theory (with $n = 3$; see Fig. 5).

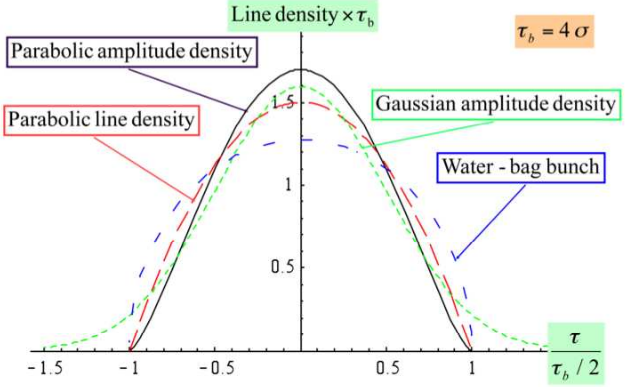

Figure 3: Longitudinal profiles of four typical (theoretical) distributions.

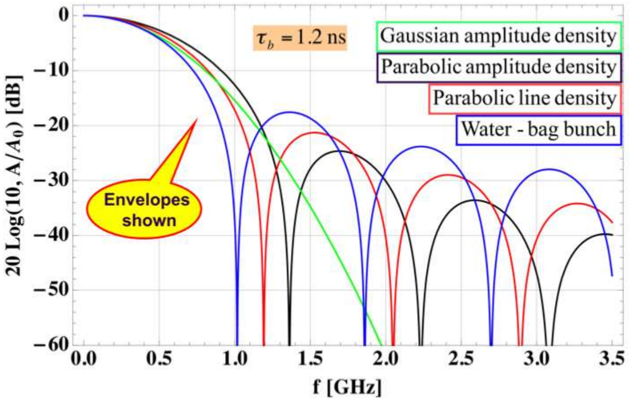

Figure 4: Power spectra corresponding to Fig. 3 (considering a full or 4-sigma bunch length of 1.2 ns).

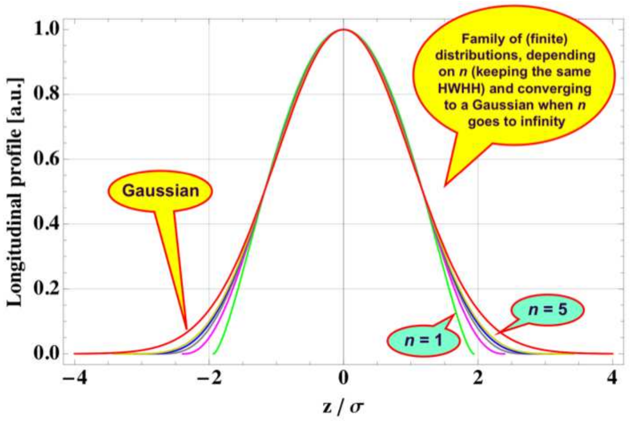

Figure 5: Family of (finite) distributions, keeping the same half width at half height, depending on the parameter n, and converging to a Gaussian distribution when n goes to infinity.

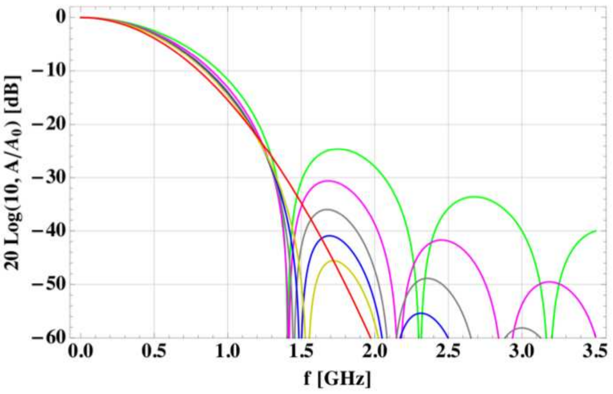

Figure 6: Power spectra corresponding to Fig. 5.

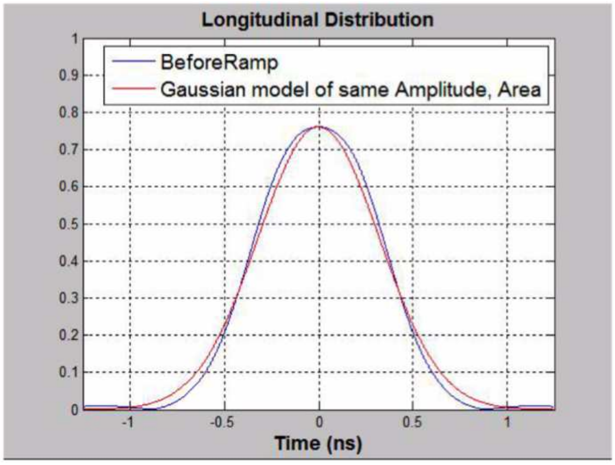

Figure 7: Longitudinal profile obtained by taking the inverse Fourier Transform of the measured spectrum before the ramp (see Fig. 2a; Courtesy of Themistoklis Mastoridis and Philippe Baudrenghien).

Consider now first the case of the Resistive-Wall impedance, and, as an example, the particular case of the LHC beam screen (neglecting the holes, whose contribution has been estimated to be small in the past, and the weld for the moment) [3]. A good approximation of the longitudinal impedance over the frequency range of interest is given by the "classical" formula

$$Z_l\left(f\right) = \left(1 + j\right)\frac{L}{2\pi b}\sqrt{\frac{\pi\, f\, \rho\, Z_0}{c}}\,, \tag{3}$$

where j is the imaginary unit, L the length of the equipment considered (approximated to the LHC circumference in this simple example, i.e. 26658.883 m), b the beam screen half height (assumed to be 18.4 mm), ρ the resistivity (assumed to be 5.5 10^{-10} Ωm for copper at 20 K), Z_0 the free-space impedance and c the speed of light. The plots of the impedance and corresponding wake function are depicted in Fig. 8. The beam power loss can

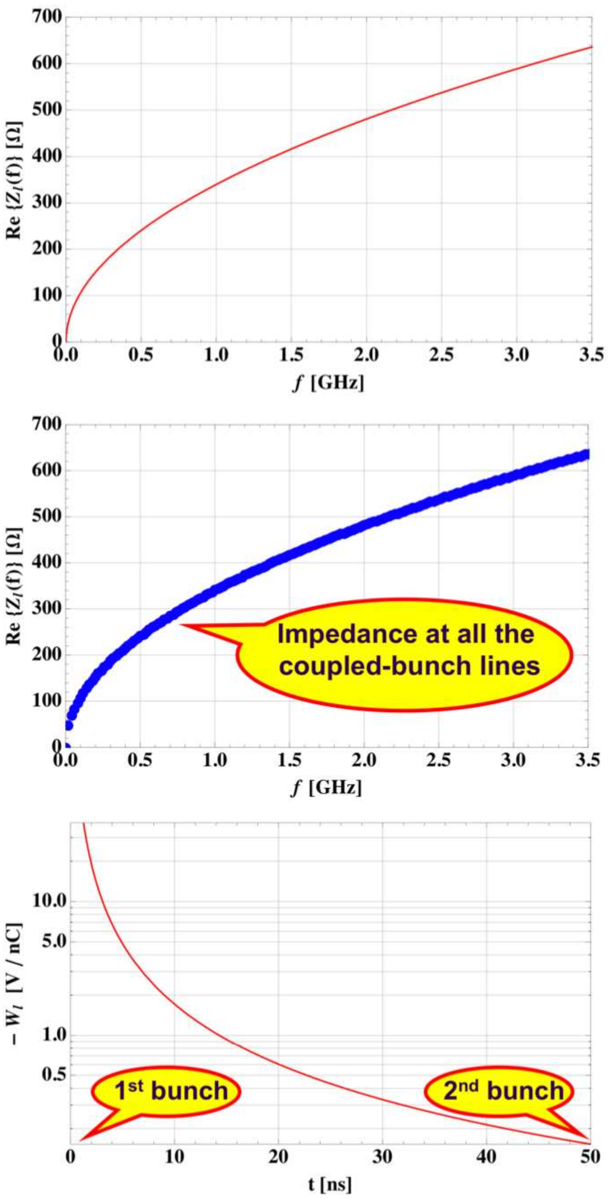

Figure 8: Resistive-Wall impedance for the case of the LHC beam screen (neglecting the holes, whose contribution has been estimated to be small in the past, and the weld for the moment) and corresponding wake function.

be written

$$P_{loss} = \frac{2\,M\,I_b^2}{\omega_0} \int_{x=0}^{\infty} f\,(\,x\,)\,dx\;, \tag{4}$$

with

$$f\,(\,p\,M\,\omega_0\,) = \mathrm{Re}\left[\,Z_l\,(\,p\,M\,\omega_0\,)\,\right] \times \mathrm{PowerSpectrum}\left[\,p\,M\,\omega_0\,\right], \tag{5}$$

$$\sum_{p=0}^{\infty} f\,(\,p\,M\,\omega_0\,) \approx \frac{1}{M\,\omega_0} \int_{x=0}^{\infty} f\,(\,x\,)\,dx\;, \tag{6}$$

$$Z_{loss} = 2\,M \sum_{p=0}^{\infty} f\,(\,p\,M\,\omega_0\,) \approx \frac{2}{\omega_0} \int_{x=0}^{\infty} f\,(\,x\,)\,dx\;. \tag{7}$$

If in addition the longitudinal bunch profile is assumed to be Gaussian, Eq. (4) can be solved analytically and the following result is obtained

$$P_{loss/m}^{G,RW,1\,\mathrm{layer}} = \frac{1}{2\pi R}\,\Gamma\!\left(\frac{3}{4}\right)\frac{M}{b}\left(\frac{N_b\,e}{2\,\pi}\right)^2 \sqrt{\frac{c\,\rho\,Z_0}{2}}\;\sigma_t^{-3/2} \tag{8}$$

$$\approx 85\ \mathrm{mW/m}\,,$$

where Γ is the Euler gamma function, the number of bunches has been assumed to be 1782 (for the 50 ns bunch spacing), the number of protons per bunch 1.4 10^{11} p/b, and the rms bunch length 0.3 ns. Assuming the real power spectrum it would give the same result within few tens of percent and for the 25 ns beam (i.e. 2 times more bunches), it would give a factor 2 more power.

If one considers now the longitudinal weld, as clearly seen in Fig. 9 [3], an estimate of the power loss from the induced currents in the weld is given by

$$\frac{P_{loss/m}^{Weld}}{P_{loss/m}^{G,RW,1\,\mathrm{layer}}} \approx \sqrt{\frac{\rho_{SS}^{20K}}{\rho_{Cu}^{20K}}} \times \frac{\Delta_l^{Weld}}{2\pi\,b} \approx 57\%\;, \tag{9}$$

with

$$\frac{\Delta_l^{Weld}}{2\pi\,b} = \frac{2}{2\pi \times 18.4} = \frac{1}{\pi \times 18.4} \approx \frac{1}{60}\,, \tag{10}$$

where $\rho_{SS}^{20K} = 6 \times 10^{-7}\ \Omega\mathrm{m}$ is the assumed resistivity of the weld (stainless steel) and 2 mm the assumed width. Therefore, even though the weld corresponds to only ~ 1/60 of the cross-section, the power loss due to the weld is not negligible at all and amounts to ~ 57 % of the power loss computed without the weld.

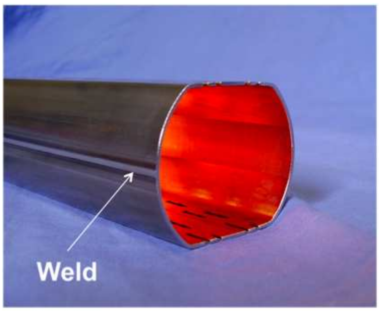

Figure 9: LHC beam screen with its longitudinal weld.

Consider now the case of a narrow resonance, describing a trapped mode due to the geometry. It is described by 3 parameters: (i) the resonance frequency, assumed to be here $f_r = 1\,\mathrm{GHz}$; (ii) a shunt impedance, assumed to be here $R_l = 10\,\Omega$; and (iii) a quality factor Q, whose value is scanned below. The impedance plots are represented in Fig. 10 together with the corresponding wake functions. It can be seen with this example that if the quality factor is bigger than ~ 100, only one line can be considered (the bunches are coupled and this is the total current which matters) whereas if the quality factor is smaller than ~ 20, then the bunches are not coupled.

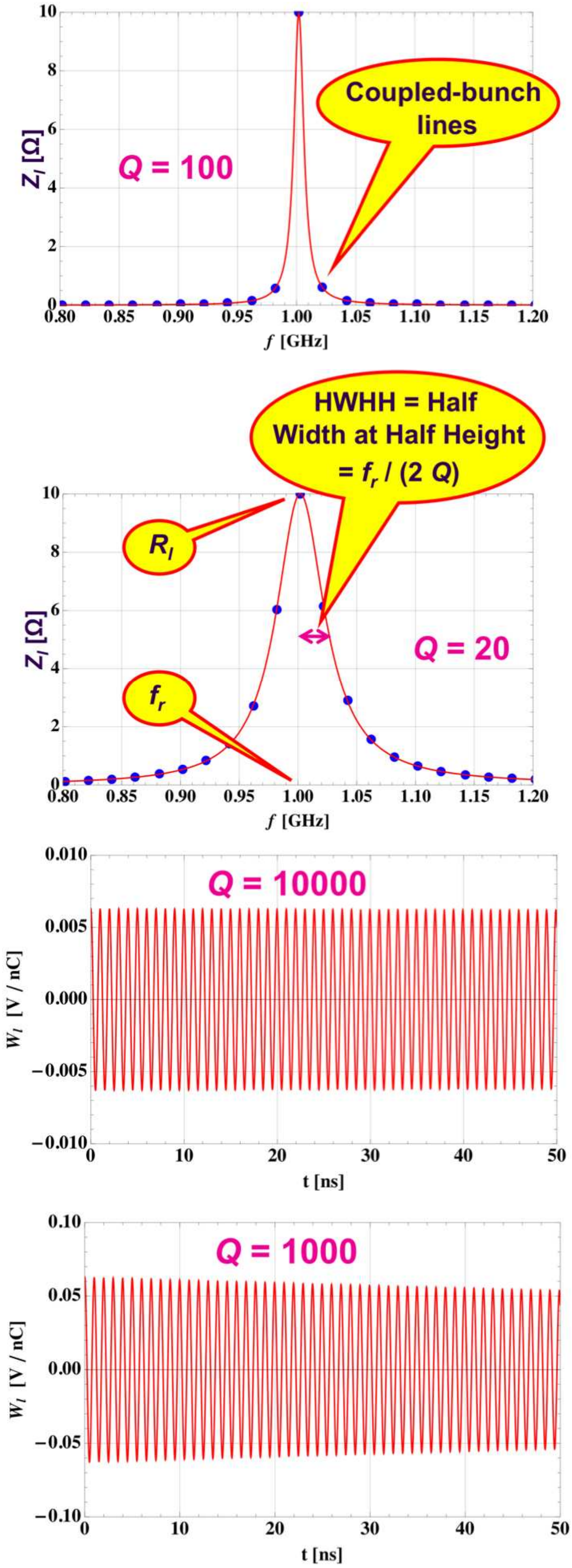

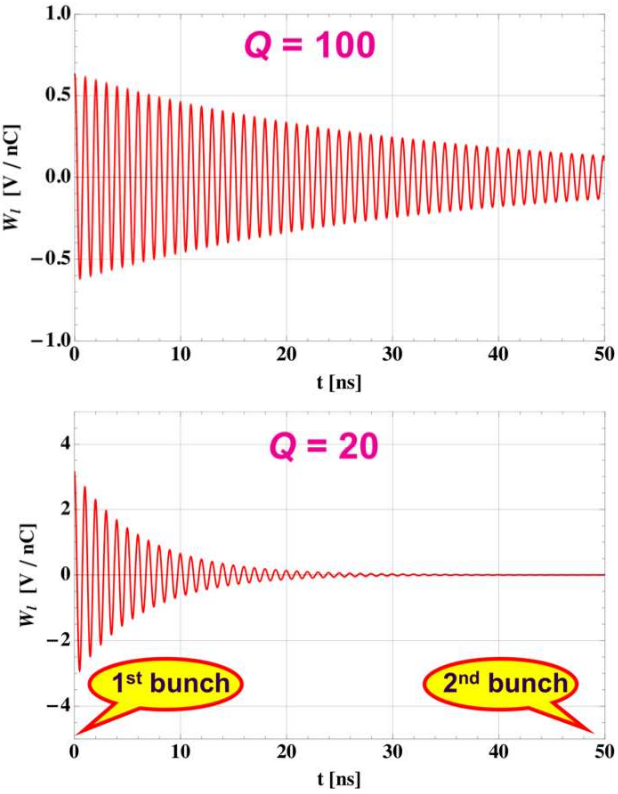

Figure 10: Impedance plots for the resonance with the resonance frequence $f_r = 1\,\text{GHz}$, shunt impedance $R_l = 10\,\Omega$, for different values of quality factors and corresponding wake functions.

In the case of a large quality factor, when only one line can be considered (assuming the worst case where the line is on top of a coupled-bunch line), a very simple equation is found for the power loss, which can be expressed as

$$P_{loss} = \left(M\, I_b \right)^2 \times R_l \times 10^{\frac{P_{dB}\left(f_r \right)}{10}} , \qquad (11)$$

where $M\, I_b$ is the total beam current and $P_{dB}\left(f_r \right)$ is the power in dB at the frequency f_r read from a power spectrum (computed or measured). Considering 1380 bunches (which was the maximum number in 2011) and $1.4\ 10^{11}$ p/b gives a total beam current of ~ 0.36 A. Assuming the previous trapped mode ($f_r = 1\,\text{GHz}$ and $R_l = 10\,\Omega$) and considering the measured power spectrum $P_{dB}\left(f_r \right) \approx -17\,\text{dB}$ (see Fig. 2c) gives a power loss of $\sim 26\,\text{mW}$. Note that in the case of a bunch with a Gaussian longitudinal profile, Eq. (11) is written

$$P_{loss}^{Gaussian} = \left(M\, I_b \right)^2 \times R_l \times e^{-\left(2\pi f_r \sigma_\tau \right)^2} , \qquad (12)$$

where σ_τ is the rms bunch length (in s).

The usual solutions to avoid or minimize the RF heating, depending on the situation, are the following:

- Increase the distance between the beam and the equipment.
- Coat the surface with a good (better) conductor.
- Close large volumes, which could lead to resonances at low frequency (i.e. more harmful), and provide smooth transitions. This explains why some beam screens, RF fingers etc. have been installed.
- Install some blocks of ferrite (not directly seen from the beam and, if possible, close to the maximum of the magnetic field of the trapped mode):
  - Adding a material with (magnetic) losses, the quality factor Q is decreased (by few tens, say 50, to give a number), while R_l / Q is conserved (depending only on the geometry);
  - Therefore, $R_{l2} = (R_{l1} / Q_1) \times Q_2$ is decreased by 50;
  - The power loss is thus decreased accordingly if Q is still sufficiently high (or less if other coupled-bunch lines are involved);
  - The ferrite should absorb the remaining (much smaller) power;
  - Note that the resonance frequency should also slightly decrease.
- Increase the bunch length (and more generally modify the longitudinal profile, i.e. the power spectrum, as it can be sometimes more complicated), but then the luminosity will decrease a bit for longer bunches through the geometric reduction factor and possible losses from the bucket will appear above a certain value (to be studied in detail). The luminosity reduction factor is given by

$$F = 1 \Big/ \sqrt{1+\left(\frac{\theta_c\,\sigma_z}{2\,\sigma^*}\right)^2}\,, \qquad (13)$$

where θ_c is the full crossing angle at the IP (Interaction Point), σ_z is the rms bunch length (in m) and σ^* is the transverse rms beam size at the IP. Several cases are plotted in Fig. 11 to see the variation of the reduction factor with the bunch length. It can be seen in particular that for 2012, increasing the bunch length from an rms value of 9 cm to an rms value of 10 cm will decrease the luminosity by ~ 2-3 %.

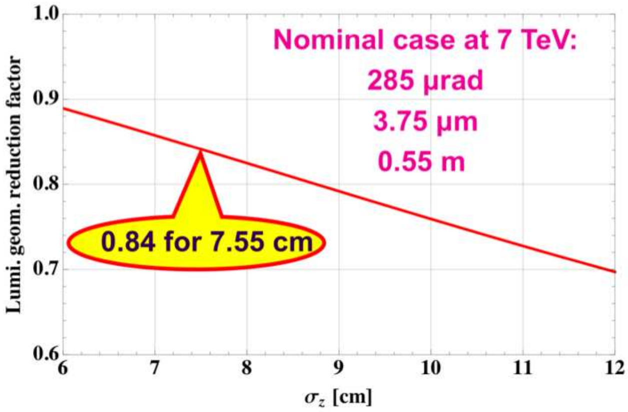

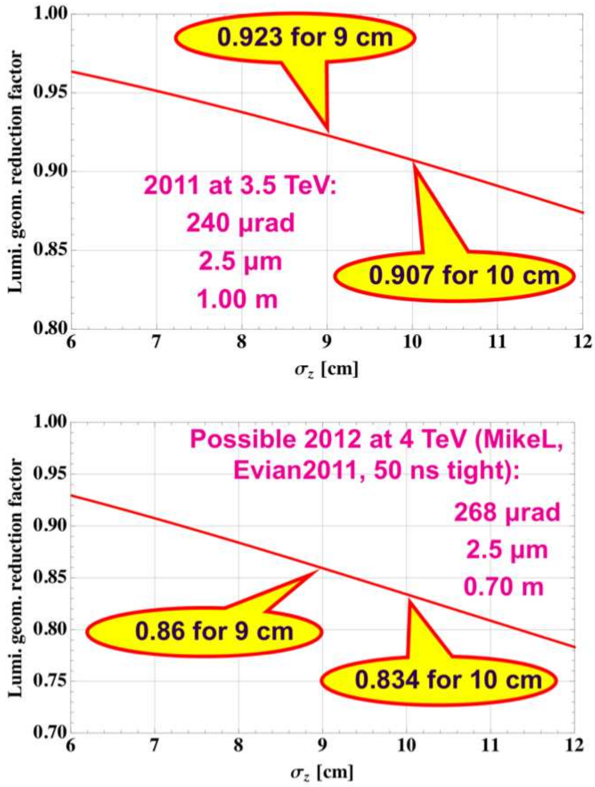

Figure 11: Luminosity reduction factor vs. bunch length for 3 sets of parameters.

Several mechanisms are in principle available for the heat transfer: conduction, convection, radiation and active coolings. As concerns convection, there is none in vacuum as there are no particles and when radiation enters into the game, the temperature is usually already quite high (note that the radiation mechanism can be improved by increasing the emissivity). Therefore, in most of the cases, only conduction remains if there are good contacts and if the thermal conductivity is good. Furthermore, in addition to these passive mechanisms, an active cooling can also be used. The LHC strategy was to use water cooling for all the near beam elements [4].

Finally, the power lost by the beam can be estimated from beam-based measurements, looking at the shift of the synchronous phase. In the absence of impedance (case 1), the bunch power gain is given by

$$\Delta P_{bunch,1} = e\,\hat{V}_{RF}\,\sin\phi_{s1}\,f_0\,N_b\,, \qquad (14)$$

where $\hat{V}_{RF}$ is the peak RF voltage and ϕ_{s1} is the synchronous phase. In the presence of an impedance (case 2), the bunch power gain is modified and the shift in power is given by

$$\begin{aligned}\Delta P_{bunch,1\rightarrow 2} &= \Delta P_{bunch,2} - \Delta P_{bunch,1} = e\,\hat{V}_{RF}\,f_0\,N_b\left(\sin\phi_{s2}-\sin\phi_{s1}\right)\\ &\approx e\,\hat{V}_{RF}\,f_0\,N_b\,\cos\phi_{s1}\,\Delta\phi_s \quad \text{with} \quad \Delta\phi_s = \phi_{s2}-\phi_{s1}\,.\end{aligned} \qquad (15)$$

Therefore, measuring the synchronous phase shift, the power loss can be deduced from Eq. (15).

“HOT” TOPICS: VMTSA, TDI AND MKI

VMTSA

In 2011, 10 modules (each of 2 bellows) were present in the machine and 8 bellows (out of 20) were found with defaults (see arrows in Fig. 12) with the spring (keeping all the fingers together around the insert) broken. Why did this happen? Is it an impedance problem? Bench impedance measurements with one wire together with electromagnetic simulations have been performed at the end of 2011 and beginning of 2012 to try and answer these questions. Some details about this equipment can be found in Fig. 13. The bench measurements corresponding to the 2 cases of Fig. 14, with on the left the correct situation and on the right a bad situation with all the bottom RF fingers in the absence of contact and with a large gap between the RF fingers and the insert, are summarized in Fig. 15. A huge resonance at ~ 200 MHz was observed when the spring jumped back (~ - 15 dB in the transmission coefficient S_{21}). It is clearly seen that when the RF fingers are in good position, this resonance disappears completely. The two other smaller resonances around 1.4 GHz are linked to something else and disappear with good contacts at the end plates (which was done for the measurements made afterwards). From the measurement of S_{21}, the longitudinal impedance can be deduced as follows [5]

$$Z_l = -2\,Z_{ch}\,\ln\left(\frac{S_{21}}{S_{REF}}\right), \qquad S_{REF} = e^{-j\,\omega\,\frac{L}{c}}, \tag{16}$$

where Z_{ch} is the characteristic impedance which was measured independently and found to be equal to

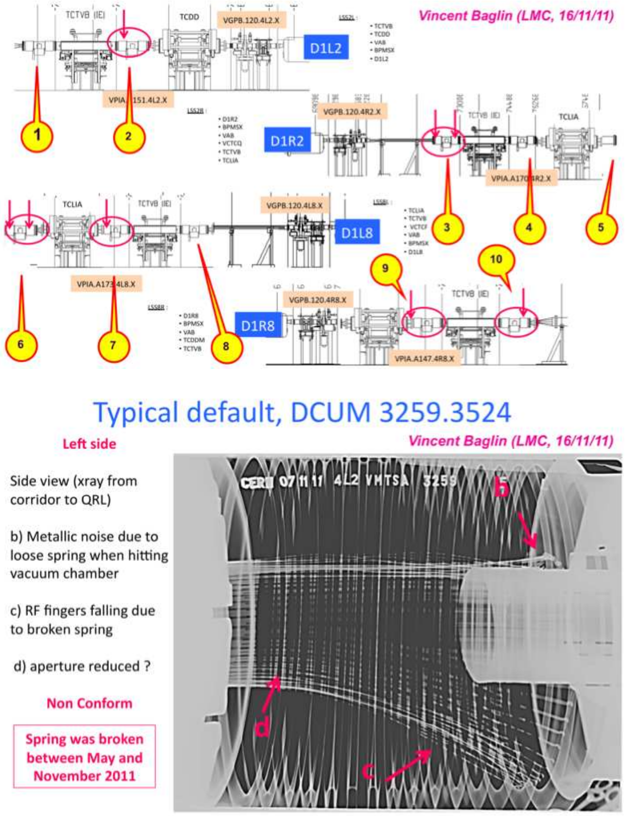
Vincent Baglin (LMC, 16/11/11)
TCTVB (IE)
TCDD
VGPB.120.4L2.X
D1L2
LSS2L
• TCTVB
• TCDD
• VAB
• BPMSX
• D1L2
VPIA.A151.4L2.X
1
2
LSS2R
• D1R2
• BPMSX
• VAB
• VCTCQ
• TCTVB
• TCLIA
D1R2
VGPB.120.4R2.X
TCTVB (IE)
TCLIA
VPIA.A170.4R2.X
3
4
5
TCLIA
TCTVB (IE)
VGPB.120.4L8.X
D1L8
LSS8L
• TCLIA
• TCTVB
• VCTCF
• VAB
• BPMSX
• D1L8
VPIA.A173.4L8.X
6
7
8
9
10
LSS8R
• D1R8
• BPMSX
• VAB
• TCDDM
• TCTVB
D1R8
VGPB.120.4R8.X
TCTVB (IE)
VPIA.A147.4R8.X
Typical default, DCUM 3259.3524
Left side
Vincent Baglin (LMC, 16/11/11)
Side view (xray from corridor to QRL)
b) Metallic noise due to loose spring when hitting vacuum chamber
c) RF fingers falling due to broken spring
d) aperture reduced ?
Non Conform
Spring was broken between May and November 2011
CERN 07 11 11 4L2 VMTSA 3259
b
c
d

Figure 12: (a) Positions of all the VMTSA present in the machine in 2012 with the ones that exhibited some issues (indicated with an arrow); (b) Typical default.

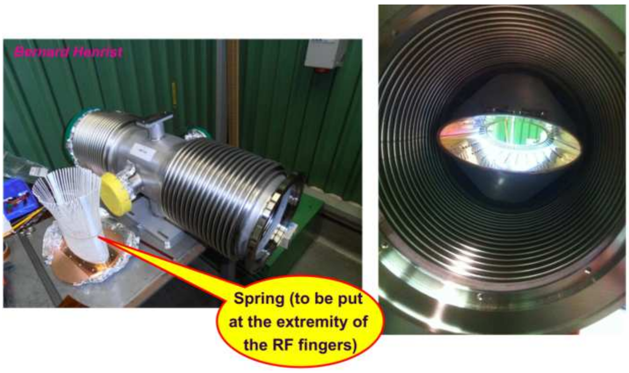
Bernard Henrist
Spring (to be put at the extremity of the RF fingers)

Figure 13: Pictures of a VMTSA (double-bellow) module with its internal insert and the RF fingers to be installed to close the large volume and avoid the big step.

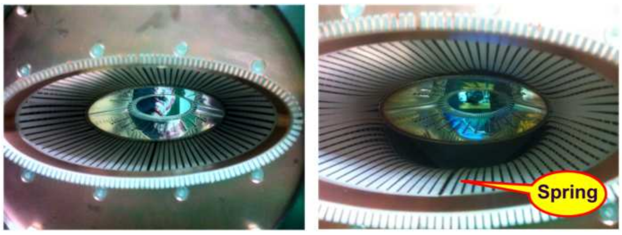

Figure 14: (Left) RF fingers correctly installed and (right) RF fingers in bad contact due to the spring, which jumped back when the VMTSA module was moved laterally by few mm (as it is supposed to work in reality).

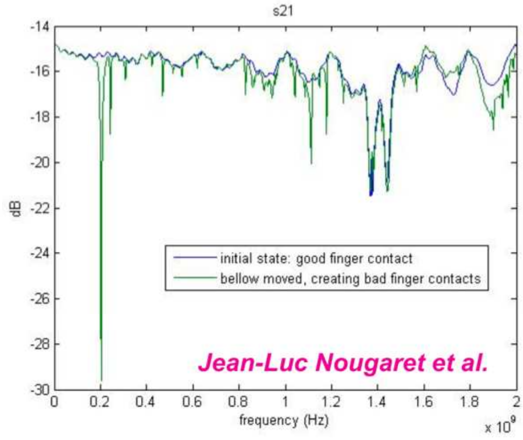

Figure 15: Transmission coefficient S_{21} in dB vs. frequency between 0 and 2 GHz for the 2 cases of Fig. 14.

~ 270 Ω. If one looks only at the real part of the longitudinal impedance (which is our case here as we are only interested in the RF heating), $S_{REF} = 1$ and the real part of the longitudinal impedance at the resonance frequency (~ 200 MHz) is

$$Z_l = -2\, Z_{ch} \ln\left(\frac{S_{21}}{S_{REF}}\right) = -2\, Z_{ch} \ln\left(10^{\frac{S_{21}[\,\mathrm{dB}\,]}{20}}\right) \approx 2 \times 270 \times \ln\left(10^{\frac{15}{20}}\right) \approx 930\,\Omega \,. \tag{17}$$

The associated power loss is thus $P_{loss} \approx 0.36^2 \times 930 \times 0.7$ ~ 85 W for 1 beam and ~ 4 × 85 = 340 W for 2 beams (worst case). The conclusion of this study is that no impedance problems are foreseen when the RF contacts are correctly installed but a huge resonance (and therefore also a huge associated heating) is observed when the RF fingers are not correctly in place as in Fig. 14 (right). Therefore, the first recommendation was and still is: try and improve the RF contacts!

TDI

The TDI is a quite involved equipment, whose main pictures are shown in Fig. 16. Two contributions to the impedance need to be taken into account: the resistive-wall (from the jaws) and the trapped modes (from the very complicated geometry). The observations made in 2011 can be summarised as follows:

- Vacuum pressure increase after ~ 1-2 h in stable beams with a maximum being reached and then a vacuum decrease:
  - Started on May 1st, 2011 for TDI.4R8,
  - Started on August 6th, 2011 for TDI.4L2.
- Heating at both extremities (measurement performed after the installation of thermocouples during a Technical Stop) on TDI.8R, by 8 to 17 deg.
- Since fill # 2219 (16/10) the TDI half gap was increased from 22 mm to 55 mm (parking position) in stable beams:
  - The vacuum pressure increase disappeared,
  - BUT, the temperature increase remained.
- Higher transverse impedances than expected from simulations and from previous measurements in 2010 (see Ref. [6]).
- Unstable position measurements, unexpected aperture restriction in P2…

Based on all these observations, a visual inspection was requested to (i) check the hBN metallization and the shielding foil (which were possible culprits for the larger impedance observed in 2011) and (ii) identify possible aperture restrictions for beam 1 between the TDI and the TCTVB left of point 2 evidenced by the aperture measurements conducted in preparation of the 2011 ion run. The conclusions of the inspection are that: (i) the Ti coating seems to be fine; (ii) a deformation of the beam screen has been observed in P8 mainly and to a smaller extent in P2 also; (iii) a soft copper was used for the beam screen instead of a copper coated stainless steel. The assumptions and predictions made in the past were the following [7]:

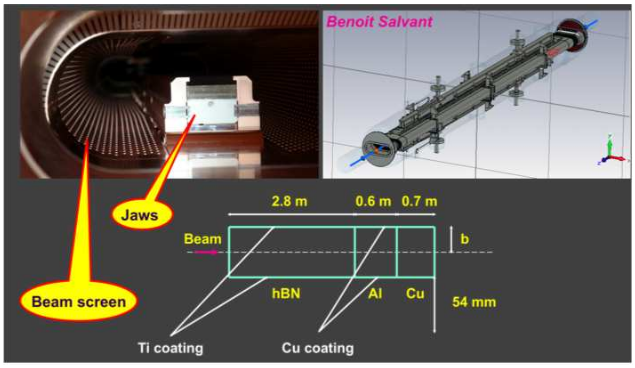

Figure 16: Some pictures of the TDI.

- Power loss due to resistive-wall (jaws): ~ 200 W.
- Water cooling present on the Al frame holding the blocks – but clamped, not brazed. Capacity 20 kW => How much cooling at block surfaces?
- Trapped modes and beam screen => Work done in the past to minimize them (simulations and measurements done with some limitations) => Not expected to be a big problem.
- No cooling of the beam screen.
- Nominal TDI operation: Should be IN only for injection (~ 20 min for nominal case) and then fully retracted (~ 55 mm half gap) => No impedance issue foreseen in the fully retracted position.

After the observation of a huge deformation of the beam screen, our impedance estimates have been reviewed using in particular the operational parameters etc. First, the power loss from resistive-wall has been re-estimated for 1380 bunches, 1.45 10^{11} p/b, 1.2 ns 4-σ bunch length and a half gap of 4.56 mm. The power loss is mainly located in the Ti coating of the hBN block. As the hBN has a very good thermal conductivity, one can assume that all the block should be heated. Scans vs. the

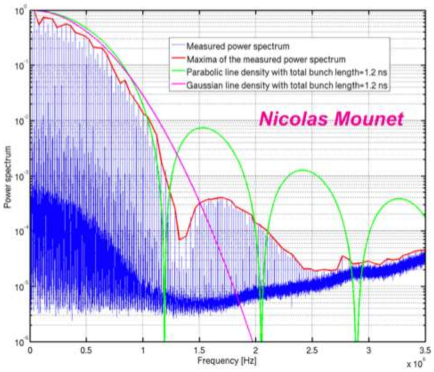

Figure 17: Measured and theoretical power spectra used for the recent TDI power loss estimates.

half-gap, the Ti thickness and the bunch length are plotted in Fig. 18, where it can be seen that ~ 300 W were expected on the hBN block at injection (with a half gap of 4.56 mm whereas 7.7 mm were considered in the past, in 2004, as well as another resistivity [7]) and about ten times less in parking position in stable beams. It also shows that the power loss decreases proportionally to the half gap, the Ti thickness and the bunch length.

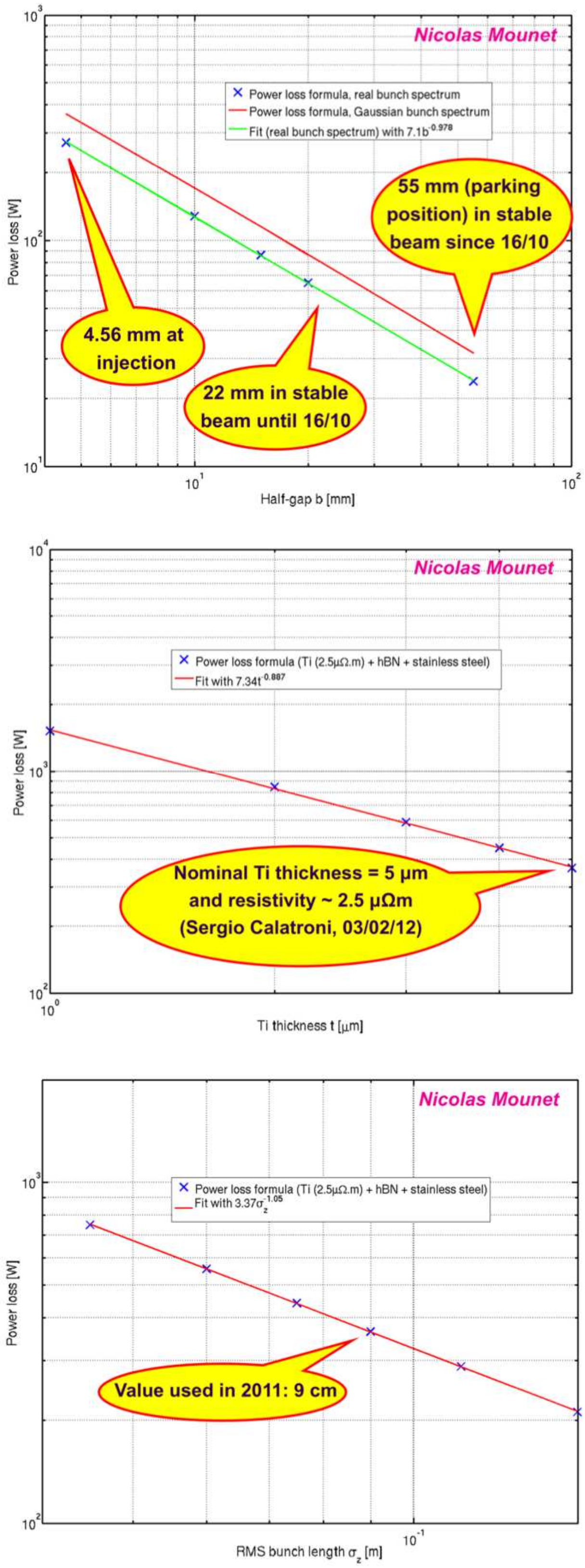

Figure 18: Scans of the TDI resistive-wall power loss versus the half-gap, the Ti thickness and the bunch length.

As concerns now the trapped modes, the power loss was estimated with the 3D model (which was not available in the past and was done in fall 2011), with more powerful computers and for a half gap of 8 mm (still work in progress). The summary of most of the trapped modes is shown in Fig. 19. Therefore, both low-frequency and high-frequency modes can be dangerous. The most critical low-frequency trapped mode is the mode with the following characteristics (see Fig. 19): $f_r \approx 59$ MHz (assumed to be on top of the coupled-bunch line at ~ 60 MHz), $R_l = 150\ \Omega$ and $Q = 195$. The associated power loss is thus $P_{loss} \approx 0.36^2 \times 150 \times 1 \approx 19.4$ W for 1 beam and $\sim 4 \times 19.4 \approx 78$ W for 2 beams (worst case). Furthermore, only ~ 20% of the power loss is expected in the beam screen. The most critical high-frequency trapped mode is the mode with the following characteristics (see Fig. 19): $f_r \approx 1227$ MHz (assumed to be on top of the coupled-bunch line), $R_l = 21000\ \Omega$ and $Q = 917$. The associated power loss is thus $P_{loss} \approx 0.36^2 \times 21000 \times 10^{-2.8} \approx 4.3$ W for 1 beam and $\sim 4 \times 4.3 \approx 17.2$ W for 2 beams (worst case). In this case, the electromagnetic fields are very localized.

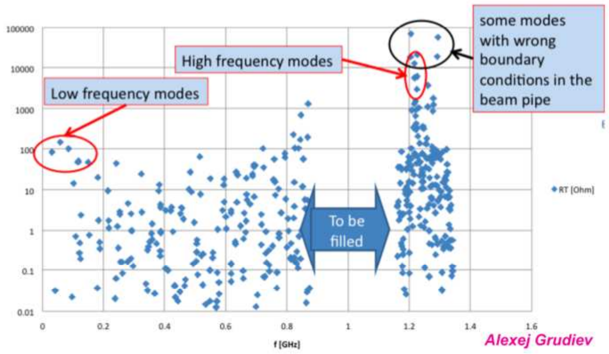

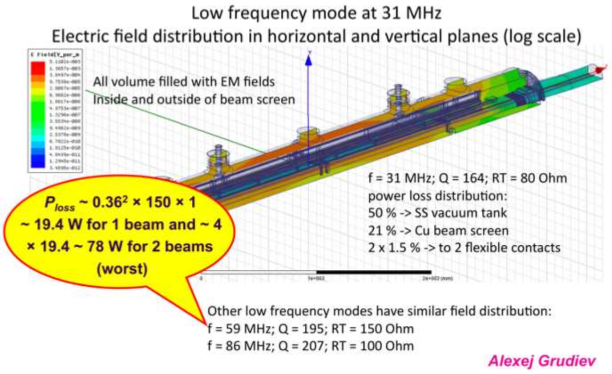
Low frequency mode at 31 MHz
Electric field distribution in horizontal and vertical planes (log scale)
All volume filled with EM fields inside and outside of beam screen
f = 31 MHz; Q = 164; RT = 80 Ohm
power loss distribution:
50 % -> SS vacuum tank
21 % -> Cu beam screen
2 x 1.5 % -> to 2 flexible contacts
Ploss ~ 0.36² × 150 × 1 ~ 19.4 W for 1 beam and ~ 4 × 19.4 ~ 78 W for 2 beams (worst)
Other low frequency modes have similar field distribution:
f = 59 MHz; Q = 195; RT = 150 Ohm
f = 86 MHz; Q = 207; RT = 100 Ohm
Alexej Grudiev

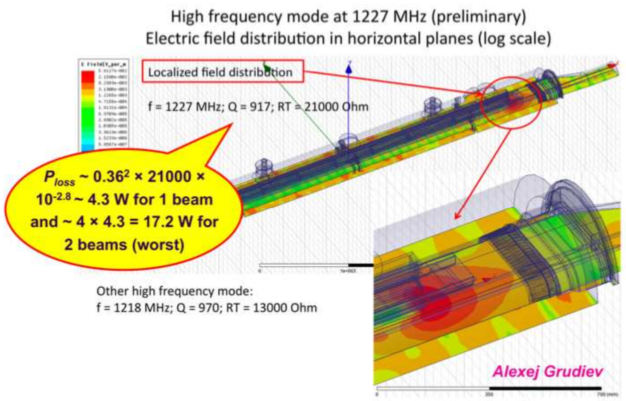
High frequency mode at 1227 MHz (preliminary)
Electric field distribution in horizontal planes (log scale)
Localized field distribution
f = 1227 MHz; Q = 917; RT = 21000 Ohm
P_{loss} ~ 0.36² × 21000 × $10^{-2.8}$ ~ 4.3 W for 1 beam and ~ 4 × 4.3 = 17.2 W for 2 beams (worst)
Other high frequency mode:
f = 1218 MHz; Q = 970; RT = 13000 Ohm
Alexej Grudiev

Figure 19: Summary of most of the TDI trapped modes (still work in progress) for a half gap of 8 mm (using the 3D model done in fall 2011).

Can these power losses in the beam screen explain the observed deformation? Assuming a simple steady-state model, where radiation in the only heat transfer mechanism between 2 infinitely long concentric cylinders, the inner one for the bean screen whose temperature has to be found and the outer one assumed to be at room temperature. It can be seen in Fig. 20 that if the beam screen is in stainless steel ~ 100 W/m are needed to reach ~ 200°C, whereas ~ 400°C can be reached in the case of a copper beam screen.

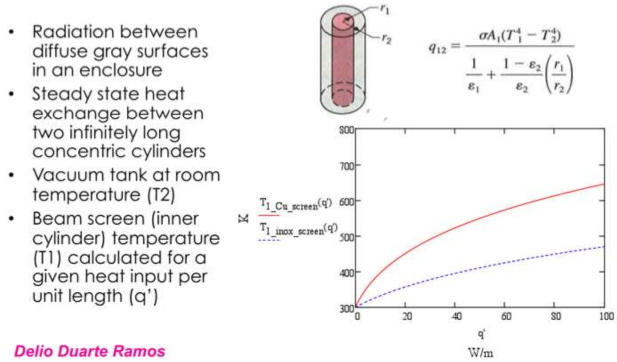

- Radiation between diffuse gray surfaces in an enclosure
- Steady state heat exchange between two infinitely long concentric cylinders
- Vacuum tank at room temperature (T2)
- Beam screen (inner cylinder) temperature (T1) calculated for a given heat input per unit length (q')

$$q_{12} = \frac{\sigma A_1 (T_1^4 - T_2^4)}{\frac{1}{\varepsilon_1} + \frac{1-\varepsilon_2}{\varepsilon_2}\left(\frac{r_1}{r_2}\right)}$$

r_1
r_2
K
$T_{1\_Cu\_screen}(q')$
$T_{1\_inox\_screen}(q')$
800
700
600
500
400
300
0
20
40
60
80
100
q'
W/m
Delio Duarte Ramos

Figure 20: Estimated beam screen temperature vs. deposited power in the beam screen (per meter), considering only radiation for the heat transfer, for both copper and stainless steel beam screens.

The power loss was estimated during some MDs through the synchronous phase shift when the TDI jaws were open and closed several times. The result of this measurement is shown in Fig. 21. An increase of the power loss of ~ 1 to 2 kW was observed (using Eq. (15)) when the TDI jaws were closed from parking position to a half gap of 4.7 mm. Furthermore, it seemed to be about linear with the number of bunches, which would mean that it is mainly dominated by a broad-band impedance (i.e. resistive-wall or a low-Q resonance?). It is worth reminding that a much smaller value was predicted for the resistive wall (~ 300-400 W), which could mean (if the synchronous phase shift measurements are reliable) that the Ti resistivity is higher than expected or the thickness is smaller. This would also explain the larger transverse impedance observed last year [6]. However, in this case the main power loss should not be in the beam screen, and cannot explain therefore the deformation… This still has to be followed up in detail.

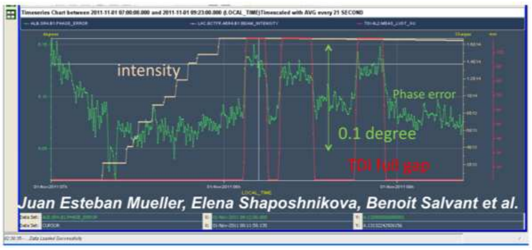
Timeseries Chart between 2011-11-01 07:00:00.000 and 2011-11-01 09:23:00.000 (LOCAL_TIME)Timescaled with AVG every 21 SECOND
intensity
Phase error
0.1 degree
TDI full gap
LOCAL_TIME
Juan Esteban Mueller, Elena Shaposhnikova, Benoit Salvant et al.
Data Set:
CURSOR
Data Loaded Successfully

Figure 21: TDI power loss estimated by measuring the synchronous phase shift as a function of the distance between the two jaws.

MKI

The MKI is also a quite involved equipment depicted in Fig. 22. All the MKIs were getting hotter and hotter during the 2011 run as can be seen in Fig. 23. Recent electromagnetic simulations (with 15 out of 24 conductive strips of the ceramic pipe) revealed a very good agreement with previous bench impedance measurements, as can be seen in Fig. 24, which gives even more confidence than before for the power loss estimates made in the past. These estimates have been updated for the nominal bunch intensity of 1.15 10^{11} p/b (it is 1.7 times bigger for 1.5 10^{11} p/b), and summarized in Table 2. It is worth reminding that the original design was

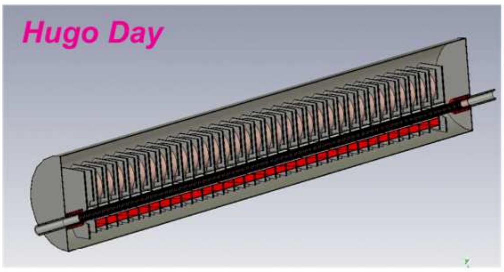

Figure 22: Picture of the LHC MKI.

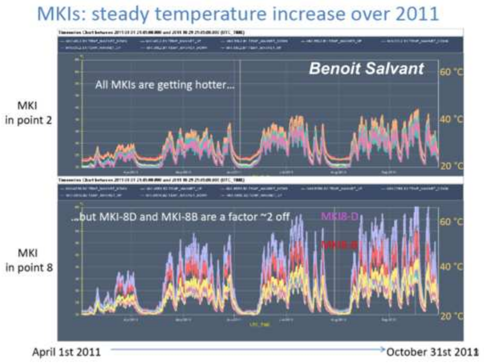

Figure 23: Evolution of the temperatures of the different MKIs during the 2011 run.

foreseen with 24 conductive strips but then the number was reduced to 15 due to HV electrical breakdowns, which had a huge impact on the longitudinal impedance and associated RF heating. The necessity of the conducting strips is also clearly revealed.

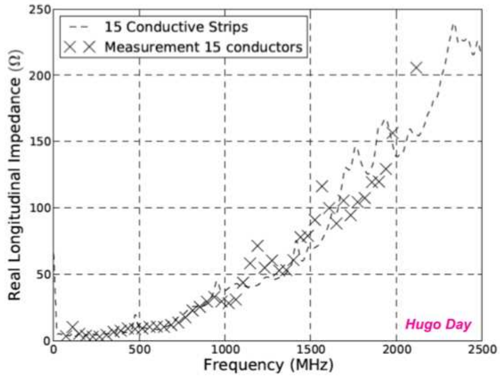

Figure 24: Comparison between past bench impedance measurements and recent electromagnetic simulations.

	25ns		50ns	
	1.1ns (W)	1.2ns (W)	1.1ns (W)	1.2ns (W)
24 Screen Conductors	44	43	17	16
15 Screen Conductors	150	133	78	68
No Screen Conductors	4817	3703	3067	2663
15 long, 9 short	138	127	69	62
No Metalisation	47660	40637	30187	27841
No Damping Ferrites	28	27	15	14
No Screen	4904	4314	3120	2745
Alt Screen 1	75	74	33	33

Table 2: MKI power loss estimates for two different bunch lengths, for both 25 ns and 50 ns beams, and for the nominal bunch intensity of 1.15 10^{11} p/b. Courtesy of Hugo Day.

LESSONS FOR 2012 (AND AFTER)

- **VMTSA**: No impedance problems are foreseen if the RF contacts are good. A task force was suggested and approved during a recent LMC meeting to review the design of all the components of the LHC equipped with RF fingers [8].
- **TDI**: The jaws should be IN only during injection (~ 20 min in nominal case) and then should be fully retracted (in parking position). Is the beam screen deformation a consequence of the impedance with small gaps? Detailed analyses are still ongoing. Can we add a Cu coating on the Ti flash as this would considerably reduce the resistive-wall impedance (if needed in particular during future scrubbing runs). Can we improve the cooling?
- **MKI**: Impedance simulations have been performed and a very good agreement with past measurements has been obtained. Therefore, there is no surprise with the impedance but we might need to wait few hours before injecting in 2012 if the beam intensity is increased or the bunch length reduced. There are current discussions to replace the MKI8D by a spare with 24 screen conductors instead of 15, during the technical stop foreseen in August 2012. This should considerably reduce the RF heating. In the future the cooling system could be improved and high-Curie temperature ferrite could be used.
- **ALFA detector (not a worry for the LHC machine but for the experiment)**: We might need to remove it for high intensity beams (as it is foreseen in the design report). However, the time needed to remove and re-install it (i.e. few days) might not be compatible with a normal technical stop (discussions still ongoing). Finally, some cooling (as TOTEM) could be installed during LS1.

REFERENCES

[1] B. Salvant et al., Beam Induced Heating, LHC Beam Operation Workshop, Evian, 12-14 December 2011.

[2] M. Furman, H. Lee and B. Zotter, Energy Loss of Bunched Beams in SSC RF Cavities, SSC-116, March 1987.

[3] E. Métral, Beam Screen Issues, Proc. of the EuCARD-AccNet-EuroLumi Workshop on The High-Energy Large Hadron Collider, Villa Bighi, Malta, 14-16 October, 2010.

[4] R. Assmann, private communication (2009).

[5] F. Caspers, Impedance Determination – Bench Measurements, Handbook of Accelerator Physics and Engineering (Edited by A.W. Chao and M. Tigner), 2nd Printing, World Scientific, 2002.

[6] Nicolas Mounet et al., Impedance Effects on Beam Stability, LHC Beam Operation Workshop, Evian, 12-14 December 2011.

[7] TDI information on the CERN LHC impedance Webpage: http://lhc-impedance.web.cern.ch/lhc-impedance/LHC_equipments.htm#TDI.

[8] LRFF (LHC RF Fingers) Task Force (to review the design of all the components of the LHC equipped with RF fingers): http://emetral.web.cern.ch/emetral/LRFF/LRFF.htm.